Pseudocapacitive random and aligned nano-porous electrode materials for supercapacitors

B. Saruhan, G.C. Mondragón Rodríguez and Y. Gönüllü

*German Aerospace Center, Institute of Materials Research, DLR-WF
Linder Hoehe, 51147 Cologne, Germany, bilge.saruhan@dlr.de

ABSTRACT

Capacitive charge-storage properties of mesoporous films made of aligned metal-oxides in core + shell architecture are superior to those of non-porous and crystalline metal-oxides. Cation intercalated, aligned nano-structured (titania) combined with redox capable oxides introduces enhanced capacitance and storage capabilities. Mn-based mixed redox oxides yield higher cyclic charge/discharge behaviour. Specific capacitance values exceeding 170 F/g have been achieved with single oxide electrodes. The half-cell electrochemical testing of the electrodes by means of three electrode configuration indicates that charge-storage and charge/discharge cycling stability can be improved by nanostructuring mesoporous structuring of the oxides.

Keywords: pseudocapacitance, manganese oxide, anodisation, titania, Li-intercalation.

1 INTRODUCTION

Batteries require long time to charge but store greater charges, while capacitors can be charged very rapidly within seconds, but suffer from lower energy densities. With new electrodes which introduce pseudo-capacitance and higher surface area, super-capacitors charge rapidly and also have higher electrical energy densities and supply this longer. These features are desirable for a range of applications, in electric vehicles and for storage of energy from renewable energy supplies such as solar and wind power which can come in short bursts. Other applications of super-capacitors and more specifically pseudo-capacitors that combine features of both rechargeable battery and standard capacitor are in mobile digital technologies and flash photography.

Supercondensators (supercaps) offer a great combination of high energy and power. Energy density of supercaps is 100 times higher than conventional condensators and the power density is 10 times higher than batteries. The challenge is to develop a material system with high surface area and low electrical conductivity.

It is prophesied that electrical energy storage systems having high energy density and high power density can be realised if pseudo-capacitance and electrostatic storage is combined. Thus, our research focuses on the development of electrode materials based on psedocapacitive oxides in order to increase the specific capacitance and energy density introduced by means of faradaic pseudo-capacitive reactions. This work demonstrates the fabrication of pseudo-capacitive mixed and doped oxide films grown by electrochemical deposition on graphite and anodic oxidised nano-tubular layers. Electrochemical deposition yields randomly distributed fine pores between the needle type of grains (Fig. 1). The electrodes having nano-tubular layers achieved by anodisation of metallic plates can be doped additionaly to increase the storage capability.

The results indicate that the optimum combination of redox oxides and the morphological aspects of the electrodes play an important role in the enhancement of the capacitance and storage capabilities.

2 EXPERIMENTAL

2.1 Synthesis of Porous Electrodes

Manganese oxide was anodic deposited on to the graphite substrates of 1 cm^2 in a $Mn(CH_3COO)_2$ solution at 25°C.

2.2 Synthesis of Nano-Tubular Electrodes

Self-standing nano-tubular TiO_2-layers were synthesized by anodic oxidation technique. Before starting anodization process, the titanium substrates were mirror polished and the Ti foils were rinsed with the de-ionized water and cleaned in an ultrasonic bath after every polishing step. The anodization of titanium substrates was carried out in an ethylene glycol (EG) -based electrolyte containing 0.3 wt. % NH_4F, and 2 vol. % H_2O and using an anodization voltage of 60V. In order to obtain Li-doped nano-tubular TiO_2-layer, the TiO_2 nanotubular layers were electrochemically doped in a 0.1 M Li^+ contained aqueous based solution under a constant current of 0.02A for 60 seconds.

2.3 Electrochemical Characterisation

Pseudo-capacitive redox-behaviour of the films is analysed by means of cyclic voltammeter measurements in

CTSI-Cleantech 2013, www.ct-si.org, ISBN 978-1-4822-0594-7

3M NaC1 solution at 25 ◦C at a potential scan rate of $20mV^{s-1}$.

Electrochemical characterization (e.g. CV, charge-discharge measurements) of un-doped and doped TiO_2-layer was carried out in a 1.0M LiCl solution by cyclic voltammetry measurements with a scanning rate of 25 mV/sec with GAMRY potentiotat.

2.4 Material Characterisation

The composition analyses were done by EDX equipped SEM for Li-doped nano-tubular TiO_2-layers and TEM for Mn-oxide. Li-doped TiO_2-layers were analyzed by glow discharge optical emission spectroscopy (GDOS) which is a surface characterization technique and mostly used to profile the elemental distributions of an alloy or compound at its thickness. GDOS uses simple DC sputtering system in order to excite the atoms in plasma. The emission intensity of excited atom has characteristic wavelengths, which can be used to determine the elemental characterization.

3 RESULTS

Two different oxide layers (Mn-oxide and Titania) with two different morphologies were produced, yielding random and eligned distributed pores.

3.1 Mesoporous MnO_2 Electrode

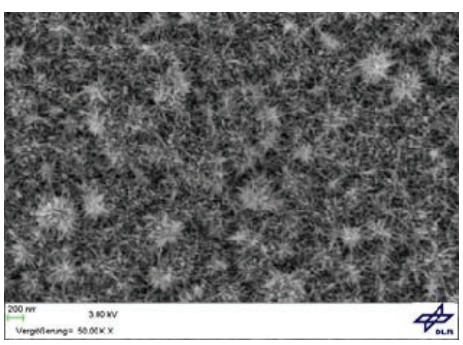

Figure 1: SEM-image of electrochemical deposited Mn-oxide-electrode.

XRD and ATEM analysis exhibit that the porous random Mn-oxide is not crystalline, although it displays a structural order similar to MnO. General morphology of this coating is needle like and very fine structured (Figs. 1 and 2). Raman measurements were carried out on Mn-oxide layer as-deposited on graphite substrate and reveal peaks Raman Shifts at 654, 368 and $311cm^{-1}$, corresponding to Mn^{2+}-O, Mn-O-Mn and out of plane bending mode of Mn-O respectively [1]. These results confirm that of the ATEM-findings that divalent manganese and a MnO-order instead of MnO_2 is present in the anodic deposited layers.

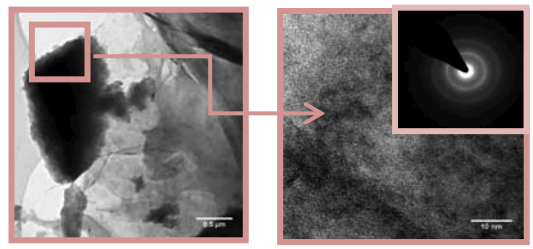

Figure 2: TEM-image of Mn-oxide layer with amorphous character.

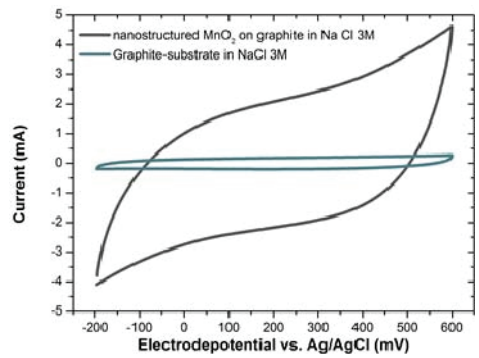

Figure 3: Current-Voltage curve of single Mn-oxide electrode measured in three-electrode configuration with a scan rate of 20mV/s in comparison with the graphite substrate having no the oxide coating (green curve).

Cyclic voltammograms (CVs) of single electrode carried out in a three-electrode cell indicate that the Mn-oxide mesoporous layer displays a larger current-potential curve, in comparison to the graphite substrate. The CV curve of the as-deposited manganese oxide is close to rectangular shapes and exhibit mirror-image characteristics as shown in Fig. 3. The results demonstrate the excellent reversibility and ideal pseudo-capacitive behaviour of the electrodes. The specific capacitances of the as-deposited oxides measured at a CV scan rate of $20mVs^{-1}$ was 170 F g^{-1}. The effect of annealing on crystallisation and the effect of crystallisation on pseudocapacitive effect will be further investigated.

3.2 Aligned Nanotubular TiO_2-Electrode

The SEM image of the Li-doped TiO_2-NTs is given in Figure 4. structure was observed after lithium-doping process. SEM analyses exhibited that the surface morphology of the Li-doped TiO_2-NTs yields the typical NTs morphology. Micro-analytic investigations by means of EDX and mapping did not yield any dopant at black TiO_2-NTs. Therefore, other analytic methods have been emplyed to identify the dopant which yields blak colour on anodic oxidised Ti surfaces after electrochemical processing in LiCl-solution.

The GDOS results proved that the nano-tubular TiO_2 -layers contain Li and the state of the lithium was monovalent (Li^+) as observed with XPS (see Figs. 5 and 6).

The results obtained with the CV-measurements of as-anodized TiO_2-NTs layers showed that in comparison with those of the bulk TiO_2-layers, a larger CV area was obtained with amorphous nano-tubular TiO_2-layers than the bulk TiO_2-layers and crystalline (anatase) nano-tubular TiO_2 layers. The amorphous nano-tubular TiO_2-layers yield not only a higher capacitance than the crystalline nano-tubular TiO_2-layer, but also their CV curve displays a different trend, yielding no clear redox peak corresponding to the intercalation and de-intercalation processes of Li^+ (Fig. 7).

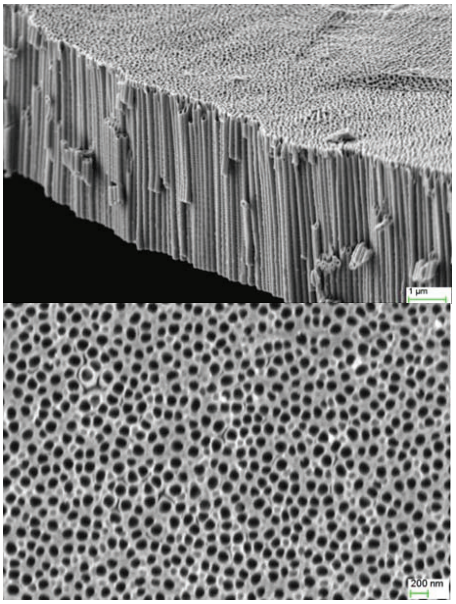

Figure 4: SEM images of nano-tubular TiO_2-layer prepared with EG based electrolyte after one-hour anodization at 60V (a) cross-section at 60V (b) top-view.

Moreover, these demonstrate that the amorphous nano-tubular TiO_2-layers yield a homogeneous insertion process (intercalation) of Li^+ at the voltage range of -0.4V and 0.4V, while the nano-tubular TiO_2-layers having anatase phase show two-redox reactions corresponding to the insertion of Li^+-ions in TiO_2 lattice (Li_xTiO_2 formation) and the extraction of Li^+-ions from TiO_2 lattice (reformation of TiO_2) [2].

The amorphous structure of the nano-tubular TiO_2 facilitates the Li-pathways relying on the structural and chemical defects in an amorphous system which do not undergo to the phase transition on the contrary to crystalline materials. The transition from tetragonal to orthorhombic phase presents internal stress in the crystalline anatase structure and thus inhibits the transfer of Li^+. Although the TiO_2 provides a highly stable anode material, the relatively low theoretical capacity of its anatase phase (168 mAh-g^{-1}) [2] is an obstacle for its enlarged employment as an anode material.

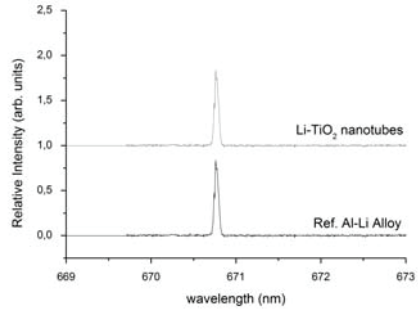

Figure 5: GDOS (top) results of Li-doped TiO_2-NTs compared with Al-Li alloy being the reference sample.-

The present results indicate that the change of the morphology from bulk to mesoporous and aligned nano-tubular will result in higher capacitance. Moreover, further processing of the nano-structured TiO_2-layers by doping with lithium improve their capacitance.

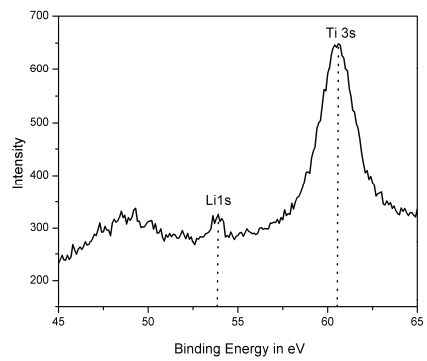

Figure 6: XPS (bottom) results of Li-doped TiO_2-NTs Al-Li alloy being the reference sample.

Literature report that, maximum discharge capacitance of the amorphous nano-tubular TiO_2-layer is approximately 0.207 mAh cm^{-2} (in the present work this measured as aprox.160 mAh cm^{-2}) and for the anatase nano-tubular TiO_2 layers it is 0.110 mAh cm^{-2} [2, 3]. With Li-doped TiO_2-NTs layers a capacitance of around 0.795 mAh cm^{-2} was obtained.

Figure 8 shows the CV curves of all studied nano-tubular TiO_2 layers. The CV curve of Li-doped nano-tubular TiO_2-layer has the largest area among the all tested nano-tubular layers. Li-doped nano-tubular TiO_2-layer shows a similar trend as amorphous nano-tubular TiO_2-layer. In this case, no redox-peaks corresponding to intercalation and de-intercalation reactions were observed after CV measurements being evidence of the homogeneous insertion/extraction process of Li^+-ions at a

voltage range between -0.4V and 0.4 V. This behaviour is similar to that of the amorphous structure.

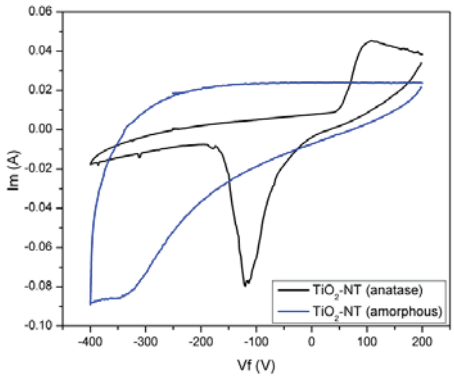

Figure 7: Cyclic voltammogragm of amorphous and anatase phase contating nano-tubular TiO_2-layers.

Charge-discharge measurements were carried out at a voltage range of 0.0 and 1.0 V in order to determine the effect of crystalline structure and doping on charge and discharge behaviour of the nano-tubular TiO_2-layers. Constant charge and discharge rates were obtained with the nano-tubular TiO_2-layer having amorphous phase. No bend-over at the charge-discharge curves was observed even after 200th cycle. This is also a clear evidence of homogeneous insertion of Li^+ in the amorphous TiO_2 nanotubes without forming a two-phase reaction between Li_xTiO_2 and TiO_2. Discharge behaviour of the amorphous nano-tubular TiO_2 was similar to the charge behaviour during all cycles, displaying no bend-over at discharge curves.

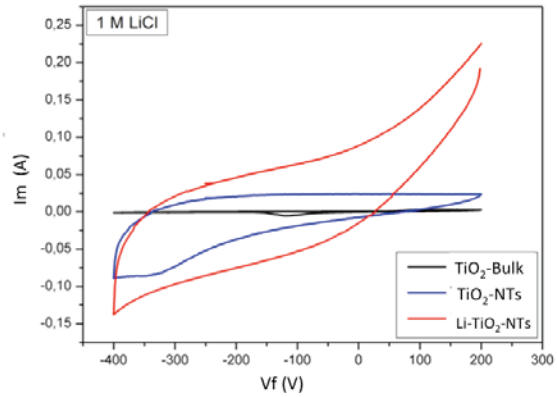

Figure 8: Cyclic voltammogram (CV) of all nano-tubular TiO_2 layers: bulk TiO_2, nano-tubular amorphous and Li-doped nano-tubular TiO_2-layers

The crystalline nano-tubular TiO_2-layers yield a different trend in the charge and discharge behaviour yielding a linear curve followed by a levelling off (Fig. 9). This behavior may be related to the insertion and extraction of Li^+-ions into the nano-tubes. The reaction is most likely due to two-phase transition to Li_xTiO_2 on deformation of TiO_2 (where x=0.5 for anatase structure) [4].

On Li-doping, constant charge and discharge rates have been observed in the amorphous layer yielding slightly bending linear curves without any voltage plateau.

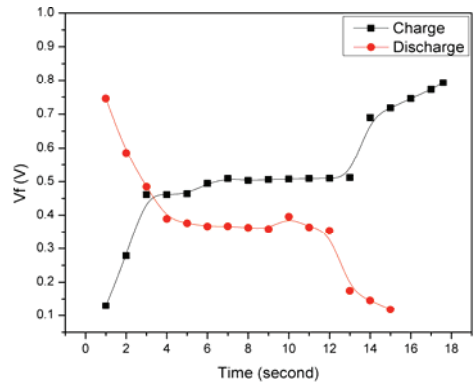

Figure 9: Charge and discharge curves of crystalline (anatase phase) nano-tubular TiO_2-layers in 1.0 M LiCl solution

4 CONCLUSIONS

Manganese oxide, with an amorphous structure and a fibrous feature, is found to consist of divalent Mn-O bonding. Cyclic voltammetry reveals that the as-deposited oxide electrodes exhibit excellent pseudo-capacitive properties. The effect of annealing on its crystallisation and pseudo-capacitive behaviour will be further investigated.

The cyclic voltammogram curves obtained after Li-doping of TiO_2 indicate that this results in transportation of Li^+ in TiO_2 lattice easier than undoped TiO_2 lattices, leading to larger CV curves. It may be that Li^+-doping in amorphous structures create a pathway or through doping introduced Li^+-ions may behave as bridges in the lattice for further Li-intercalation process.

REFERENCES

[1] C. Julien, M. Massot, S. Rangan, M. Lemal and D. Guyomard, J. Raman Spectrosc.; 33: 223- 228 (2002).

[2] W.-H. Ryu, et al., Electrochimica Acta, 61, p. 19-24 (2012).

[3] Gerhard Nuspl, K.Y., J. Mater. Chem., 7(12): p. 2529-2536 (1997).

[4] J. Wang, J. Lim, and B. Dunn, J. Phys. Chem. C, 11: p. 14925-14931(2007).